Experimental Gerontology 180 (2023) 112270

Contents lists available at ScienceDirect

Experimental Gerontology

journal homepage: www.elsevier.com/locate/expgero

Attenuation of pulmonary damage in aged lipopolysaccharide-induced inflammation mice through continuous 2 % hydrogen gas inhalation: A potential therapeutic strategy for geriatric inflammation and survival

Toshiyuki Aokage [a,b,*], Masumi Iketani [b], Mizuki Seya [a], Ying Meng [a], Kohei Ageta [a], Hiromichi Naito [a], Atsunori Nakao [a], Ikuroh Ohsawa [b]

[a] Department of Emergency, Critical Care and Disaster Medicine, Okayama University Graduate School of Medicine, Dentistry and Pharmaceutical Sciences, Okayama, Japan
[b] Biological Process of Aging, Tokyo Metropolitan Institute for Geriatrics and Gerontology, Tokyo, Japan

ARTICLE INFO

Section Editor: Daniela Frasca

Keywords:
LPS-induced inflammation
Elderly sepsis
Lipopolysaccharide
Aged mouse
Senescence-related markers
Molecular hydrogen
Hydrogen gas inhalation

ABSTRACT

Introduction: With the global population aging, there is an increased prevalence of sepsis among the elderly, a demographic particularly susceptible to inflammation. This study aimed to evaluate the therapeutic potential of hydrogen gas, known for its anti-inflammatory and antioxidant properties, in attenuating inflammation specifically in the lungs and liver, and age-associated molecular markers in aged mice.
Methods: Male mice aged 21 to 23 months, representative of the human elderly population, were subjected to inflammation via intraperitoneal injection of lipopolysaccharide (LPS). The mice were allocated into eight groups to examine the effects of varying durations and concentrations of hydrogen gas inhalation: control, saline without hydrogen, saline with 24-hour 2 % hydrogen, LPS without hydrogen, LPS with 24-hour 2 % hydrogen, LPS with 6-hour 2 % hydrogen, LPS with 1-hour 2 % hydrogen, and LPS with 24-hour 1 % hydrogen. Parameters assessed included survival rate, activity level, inflammatory biomarkers, and organ injury.
Results: Extended administration of hydrogen gas specifically at a 2 % concentration for 24 h led to a favorable prognosis in the aged mice by reducing mRNA expression of inflammatory biomarkers in lung and liver tissue, mitigating lung injury, and diminishing the expression of the senescence-associated protein p21. Moreover, hydrogen gas inhalation selectively ameliorated senescence-related markers in lung tissue, including C-X-C motif chemokine 2, metalloproteinase-3, and arginase-1. Notably, hydrogen gas did not alleviate LPS-induced liver injury under the conditions tested.
Conclusion: The study highlights that continuous inhalation of hydrogen gas at a 2 % concentration for 24 h can be a potent intervention in the geriatric population for improving survival and physical activity by mitigating pulmonary inflammation and modulating senescence-related markers in aged mice with LPS-induced inflammation. This finding paves the way for future research into hydrogen gas as a therapeutic strategy to alleviate severe inflammation that can lead to organ damage in the elderly.

1. Introduction

Global aging has led to an increase in elderly patients with sepsis (Imaeda et al., 2021). Because the elderly have less resistance to pathogens due to age-related physiological changes, infection can easily spread throughout their bodies; therefore, excess inflammation can be induced, affecting the senescent cells, and injure their organs and eventually, lead to multiple organ failure (Kotfis et al., 2019). Reduced immune cell function, termed "immunosenescence" and the accompanying increase in cellular senescence, contributes to the age-related decline in pathogen resistance (Accardi and Caruso, 2018). Furthermore, inflammation and oxidative stress are known to promote cellular senescence (de Magalhães and Passos, 2018; Dumont et al., 2000). Senescent cells continuously secrete or induce cytokines, chemokines, growth factors, and proteases to communicate with the immune system, and consequently, facilitate the pathogenesis of chronic inflammation,

* Corresponding author at: Department of Emergency, Critical Care and Disaster Medicine, Okayama University Graduate School of Medicine, Dentistry and Pharmaceutical Sciences, 2-5-1 Shikata-cho, Kita-ku, Okayama-shi, Okayama 700-8558, Japan.
E-mail address: t_aokage@okayama-u.ac.jp (T. Aokage).

https://doi.org/10.1016/j.exger.2023.112270
Received 24 June 2023; Received in revised form 8 August 2023; Accepted 9 August 2023
Available online 15 August 2023

which is one of the key factors influencing aging-related organ fibrosis and organ dysfunction (de Magalhães and Passos, 2018; Franceschi and Campisi, 2014).

Although inflammation is a cause of progressing organ dysfunction in patients with sepsis, particularly in the elderly, the effect of immunosuppressive treatments against sepsis such as corticosteroids remains controversial (Venkatesh et al., 2018). These treatments, because of their strong side effects, can be used only in severe cases and are not indicated for minor cases. Therefore, in the context of an aging population, minimally invasive treatments targeting excess inflammation and preventing the progression of cellular senescence and organ damage are needed.

Molecular hydrogen has been proven to inhibit organ damage in septic patients by exerting its anti-inflammatory and antioxidant effects. Importantly, this holds promise for addressing the specific challenges posed by severe inflammation in the elderly population. Previous studies have shown protective effects not only for cerebral infarction (Ohsawa et al., 2007) and ischemia-reperfusion (Yamamoto et al., 2020), but also for lung injury induced by hyperoxia (Kawamura et al., 2013), and hemorrhagic shock (Kawamura et al., 2013), as well as bleomycin-induced lung fibrosis (Aokage et al., 2021; Gao et al., 2019). However, there is a critical need to understand its effects on senescence-related pathways and organ injuries in the context of aging. Iketani et al. showed that drinking hydrogen-saturated water ameliorated hepatic injury induced by experimental severe inflammation induced by intraperitoneal administration of 30 mg/kg of lipopolysaccharide (LPS) in mice (Iketani et al., 2017). However, their study used seven-week-old young mice and did not assess lung injury. In the real world, previous studies cannot be directly applied to clinical patients because of the unique physiological conditions of the elderly as the primary population affected by sepsis. Furthermore, the duration and concentration of hydrogen gas inhalation needed to target inflammation and senescence in an aged population have not been well studied in the previous literature.

We conducted a new animal experiment tailored to the geriatric population to complement the previous study on subject age, endpoints, and conditions. Inhalation was selected as the molecular hydrogen delivery method in this study. This choice was made as inhalation is particularly relevant for elderly patients, who are often in an acute stage of sepsis where intestinal tract functions are impaired, and hydrogen administered through drinking water or intragastric methods may not be properly absorbed.

The aims of this study were not only to find the effect of hydrogen gas inhalation on severe inflammation that can lead to organ damage in the elderly but also to evaluate its impact on cellular senescence, which is particularly pertinent in the aging population. We aimed to clarify the optimal duration and concentration of hydrogen gas inhalation necessary for tackling both inflammation and senescence. Additionally, we studied the effects of hydrogen on senescence biomarkers in lung and liver tissue induced by LPS-induced inflammation in 21 to 23-month-old mice, thus focusing on an age group that simulates the human elderly population.

By concentrating on the aging aspect and the role of cellular senescence in severe inflammation, this study aims to provide insights that are directly applicable to the geriatric population. Although this study focuses on the LPS-induced inflammation model, which is not influenced by infection, and therefore cannot be directly applied to infection-mediated sepsis, this focus remains critical given the global aging trends and the corresponding increase in the prevalence of sepsis among the elderly.

2. Materials and methods

2.1. Animals

Twenty-one- to 23-month-old C57BL/6 male mice (42.7 ± 6.5 g, specific-pathogen free) were bred at and supplied by an animal facility in the Tokyo Metropolitan Institute for Geriatrics and Gerontology. Mice were kept on a 12-hour light/dark cycle at 22 °C to 24 °C and fed sterile food and water. Every effort was made to minimize the number of experimental animals and minimize pain or distress during the experimental procedures. All protocols followed the principles of laboratory animal care (NIH Publication No. 86-23, revised 1985), and all research protocols were reviewed and approved by the Animal Care and Use Committee of the Tokyo Metropolitan Institute of Gerontology (No.19009, No.22001). This study was conducted in compliance with the ARRIVE guidelines (https://arriveguidelines.org/). Animal conditions were checked twice daily after the administration of LPS. Dying animals that met humane endpoint criteria were euthanized by a skilled researcher using cervical dislocation. Before scheduled sampling, animals were sacrificed by exsanguination under deep anesthesia with intraperitoneal administration of 0.75 mg/kg medetomidine hydrochloride (Domitor, Meiji Seika Pharma, Tokyo, Japan), 4 mg/kg midazolam (Dormicum, Astellas Pharma, Tokyo, Japan), and 5 mg/kg butorphanol (Vetorphale, Meiji Seika) as previously described (Kawai et al., 2011). All lobes of the right lungs were removed *en bloc*, and immediately snap-frozen using liquid nitrogen to preserve their state, then stored at −80 °C until use. For further processing, the frozen right lungs were carefully ground into a powder under continuous maintenance of the frozen state with liquid nitrogen to prevent any thawing. Powdered lung tissue (30 mg) was used for RNA extraction for reverse transcription (RT)-PCR. Left lungs were used for histopathological analysis.

2.2. Generation of LPS-induced inflammation model and inhalation of hydrogen gas

The study was conducted using a mouse model of LPS-induced inflammation (Iketani et al., 2017). In summary, 1.25 mg/kg of LPS (O127:B8, Sigma-Aldrich, St. Louis, MO), which was dissolved in normal saline to 125 μg/mL concentration, was intraperitoneally injected into mice by a skilled technician with a 27-gauge needle and minimal pain. It resulted in the spillover of inflammation from the abdominal cavity to the entire body, eventually leading to severe inflammation. In sham controls, normal saline without LPS was administered in the same manner. We conducted a preliminary survival and lung histological assessment, which confirmed that at a dose of 1.25 mg/kg of LPS, survival was 80 % at the time point of 24 h and histological changes of lung injury were found.

To administer gas inhalation, three gas mixtures were supplied in a sealed acrylic gas chamber (L 40 cm × W 20 cm × H 20 cm), and the rearing cage was placed inside. Each chamber housed a maximum of four mice. The three different gas mixtures were created using prefilled cylinders of 4 % hydrogen/96 % nitrogen, 2 % hydrogen/98 % nitrogen, 100 % nitrogen, and 100 % oxygen (Taiyo Nissan, Tokyo, Japan): 1) 1 L/min of 2 % hydrogen gas mixture, which was created by mixing 0.5 L/min of 4 % hydrogen gas /96 % nitrogen and 0.5 L/min of 100 % oxygen, 2) 1 L/min of 1 % hydrogen gas mixture, which was created by mixing 0.5 L/min of 2 % hydrogen gas/98 % nitrogen and 0.5 L/min of 100 % oxygen, and 3) 1 L/min of nitrogen/oxygen gas mixture, which was created by mixing 0.5 L/min of 100 % nitrogen and 0.5 L/min of 100 % oxygen. For gas administration in the sealed acrylic chamber, temperature (acceptable range 22–24 °C) and humidity (acceptable range 40–70 %) were monitored. To confirm the efficiency of ventilation, we measured the levels of carbon dioxide and ammonia at the chamber's outlet, yielding concentrations of 2754 ± 302 ppm (average ± standard deviation) and <0.1 ppm, respectively.

Mice were assigned to eight experimental groups (see Fig. 1A): 1) the control group (C, n = 14) where after saline administration, mice were placed back into their usual cages without the airtight chamber; 2) the saline administration and non-hydrogen treatment group (SA group, n = 21), where after saline administration, mice were placed into a sealed

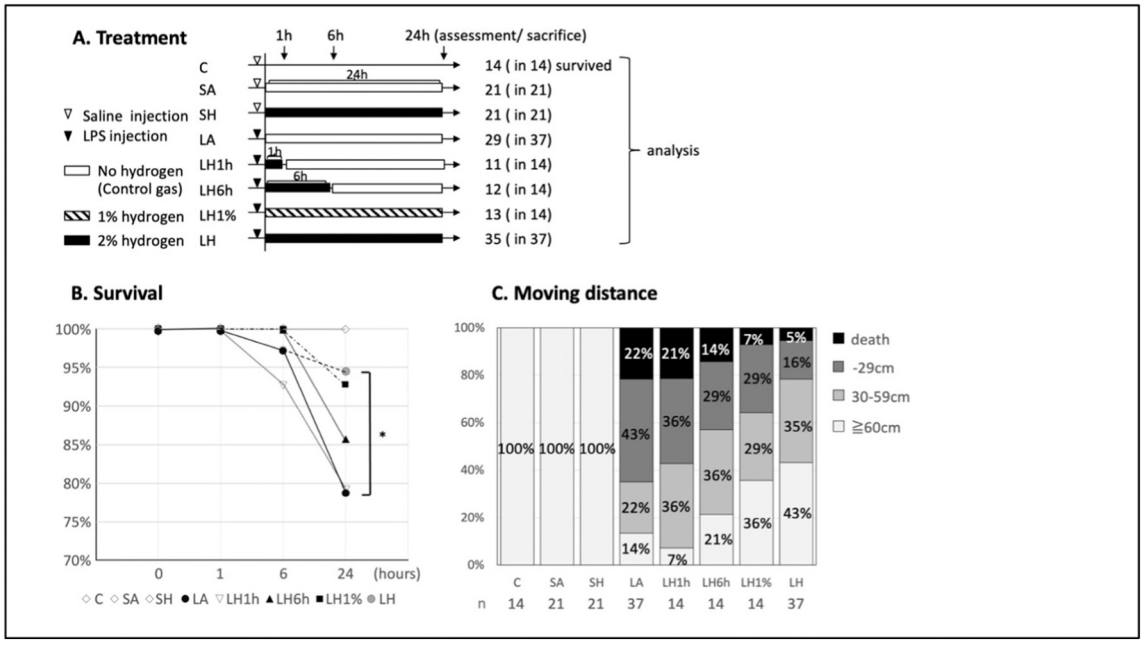

Fig. 1. Survival and movement distance under hydrogen gas inhalation in aged LPS-induced inflammation mice.
(A) Schematic diagram of the hydrogen gas inhalation administration protocol used in our aged LPS-induced inflammation mice. C indicates no treatment group; SA indicates sham without hydrogen gas inhalation; SH indicates sham with 2 % hydrogen gas inhalation; LA indicates lipopolysaccharide (LPS) administration without hydrogen gas inhalation; LH1h indicates LPS administration with one-hour hydrogen gas inhalation; LH6h indicates LPS administration with six-hour hydrogen gas inhalation; LH1% indicates LPS administration with 1 % hydrogen gas inhalation for 24 h; LH indicates LPS administration with 2 % hydrogen gas inhalation for 24 h. (B) The rate of mouse survival in the LPS-induced inflammation model at the time points of 1 h, 6 h, and 24 h after LPS or saline intraperitoneal administration. After LPS administration, survival rates were significantly improved in the LH group compared to the LA group (*$p < 0.05$). (C) Movement distance in the LPS-induced inflammation model at 24 h after intraperitoneal LPS or saline administration. Black box indicates the rate of mortality. Deep gray box indicates rate of distance below 29 cm/min. Light gray box indicates rate of distance between 30 and 59 cm/min. White box indicates movement distance rate of over 60 cm/min. The rate of movement distance below 29 cm/min in the LA group was significantly higher than that in the LH group ($p < 0.05$), and the rate above 60 cm/min in the LA group was significantly lower than that in the LH group ($p < 0.01$).

chamber with the nitrogen/oxygen gas mixture; 3) the saline administration and 2 % hydrogen treatment group (SH group, n = 21), where after saline administration, mice were placed into an airtight chamber with the 2 % hydrogen gas mixture; 4) the LPS administration and non-hydrogen treatment group (LA group, n = 34), where after LPS administration, mice were placed into an airtight chamber with the nitrogen/oxygen gas mixture; 5) the LPS administration and 2 % hydrogen treatment group (LH group, n = 34), where after LPS administration, mice were placed into an airtight chamber with the 2 % hydrogen gas mixture; 6) the LPS administration and six-hour hydrogen treatment group (LH6h group, n = 14), where after LPS administration, mice were placed into a gas chamber with the 2 % hydrogen gas mixture for 6 h, after which the 2 % hydrogen gas mixture was replaced with the nitrogen/oxygen gas mixture for 18 h, 7) the LPS administration and one-hour hydrogen treatment group (LH1h group, n = 14), where after LPS administration, mice were placed in a gas chamber with the 2 % hydrogen gas mixture for 1 h, after which the 2 % hydrogen gas mixture was replaced with the nitrogen/oxygen gas mixture for 23 h; and 8) the LPS administration and 1 % hydrogen treatment group (LH1% group, n = 14), where after LPS administration, mice were placed into an airtight chamber with the 1 % hydrogen gas mixture.

2.3. Assessment of moving distance

Mouse movement distances were examined using an open field activity test 24 h after LPS infusion. The mice were placed in square space separated by walls (L 40 cm × W 40 cm × H 26 cm) and their actions were recorded for 1 min with a video camera. The mouse movement paths were traced manually and movement distance was measured.

Movement distances were classified into four categories: 1) death, 2) <29 cm, 3) 30 cm to 59 cm, and 4) 60 cm and more. The selection of these thresholds (30 cm and 60 cm) was based on the tertiles of the distribution of total movement distances observed in mice post-LPS administration. The number of mice in each category was recorded as a percentage of the total number of mice.

2.4. Blood serum analysis

The mice were euthanized by exsanguination. A blood sample was carefully taken from the right ventricular cavity using a 21G needle and heparinized using a 1 mL syringe under deep anesthesia as described above. Whole blood was stored at room temperature for 30 min, then centrifuged at 5000 rpm for 5 min for serum separation. The blood serum was stored in a − 80 °C freezer and later used for analysis of interleukin-6 (IL6), aspartate aminotransferase (AST), alanine aminotransferase (ALT), and lactate dehydrogenase (LDH). IL6 level was analyzed using a Mouse IL-6 Quantikine ELISA Kit M-6000B (R&D Systems, Inc., Minneapolis, MN). AST and ALT were analyzed with a Transaminase CII test Wako kit (Fujifilm, Co., Tokyo, Japan). LDH was analyzed with a N-assay L LDH kit (Nittobo, Tokyo, Japan).

2.5. Hematoxylin and eosin staining

The left lungs and right lateral hepatic lobes were fixed with 4 % paraformaldehyde, dissolved in phosphate buffered saline (PBS) for two days, embedded in paraffin, and then sliced into 4-μm sections. Hematoxylin and eosin (HE) staining was performed using standardized protocols by skilled technicians in the Geriatric Pathology department at the Tokyo Metropolitan Institute of Gerontology. Images were automatically captured using the Nano-Zoomer 2.0RS slide scanner (Hamamatsu

Photonics, Shizuoka, Japan) and analyzed using NDP.view2 software, (Hamamatsu Photonics, Shizuoka, Japan). Ten high-magnification images (total magnification × 400) of HE-stained tissue were captured randomly from one slice and evaluated, using the lung injury score (Belperio et al., 2002) to quantitate the extent of histologic lung injury, which was determined based on alveolar congestion, hemorrhage, infiltration or aggregation of neutrophils in the airspace or the vessel walls, and thickness of alveolar wall/hyaline membrane formation. Each of these four items was scored (0–4) as follows: 0, normal lungs; 1, mild damage; 2, moderate damage; 3, severe damage; and 4, maximal damage.

2.6. SYBR green two-step, real-time reverse transcriptase polymerase chain reaction

The right lungs and right median hepatic lobes were frozen in liquid nitrogen immediately after collection and freeze pulverized. Messenger RNA (mRNA) levels for IL6, CD14, IκBα, p16/Ink4a, p21, C-X-C motif chemokine 2 (CXCL2), metalloproteinase-3 (MMP3), arginase-1 (ARG1), and ribosomal protein L4 (RPL4) were assessed using SYBR green two-step, real-time RT-PCR. RNA extraction was performed with the Nucleospin® RNA kit (Takara Bio Inc., Kusatsu, Japan) using powdered lung and hepatic tissue (30 mg) according to the manufacturer's instructions. Total RNA (1 μg) was reverse transcribed with ReverTraAce® qPCR RT Master Mix (TOYOBO Inc., Osaka, Japan). The mixture for SYBR Green PCR was prepared using THUNDERBIRD NEXT SYBR qPCR MIX (TOYOBO Inc., Osaka, Japan) and primers (Fasmac Co., Ltd., Kanagawa, Japan). Primer sequences are listed in Table 1. The thermal cycling protocol activated the polymerase for 10 min at 95 °C, followed by 40 cycles of 95 °C for 5 s and 60 °C for 30 s in a QuantStudio Realtime PCR machine (Thermo Fisher Scientific, Waltham, Massachusetts).

2.7. Immunohistochemistry

Paraffin-embedded lung tissue sections (4 μm) were immunostained for cleaved caspase-3 and IL6 using an ABC Kit (Vector laboratories INC., Burlingame, California). Sections were deparaffinized, rehydrated, and treated for antigen retrieval with 10 mM citric acid pH 6.0 at 120 °C for 10 min in a pressure cooker. Endogenous peroxidase inhibition was performed with 0.3 % hydrogen peroxide in PBS for 20 min at room temperature. Blocking treatment was performed with 10 % goat serum in tris buffered saline with 0.1 % Tween 20 (TBS-T) to prevent non-specific binding of antibodies. The primary antibodies (anti-cleaved caspase-3 antibody #9664 Cell Signaling Technology, Danvers, MA, dilution 1:1000; anti-interleukin-6 antibody, ab9324 Abcam, Cambridge, UK, dilution 1:1000) were diluted by Can Get Signal immunostaining Solution A (Toyobo, Osaka, Japan), applied to the sections, incubated overnight at 4 °C, and then washed with TBS-T. Biotin-conjugated secondary antibodies (anti-rabbit IgG labeling biotin 115-065-144; anti-mouse IgG labeling biotin 115-065-146, Jackson ImmunoResearch Inc., West Grove, PA, dilution 1:1000) were diluted by Can Get Signal immunostaining Solution A, applied on the sections, and incubated for 2 h at room temperature. After washing, ABC reagent was applied to the sections and then incubated for 30 min at room temperature, per the manufacturer's instructions. For 3,3′-diaminobenzidine (DAB) staining, one DAB tablet (10 mg per tablet, FUJIFILM Wako Pure Chemical Corporation, Osaka, Japan) was dissolved in 50 mL of 50 mM Tris-HCl buffer pH 7.6 with 10 μL of 30 % hydrogen peroxide, per the manufacturer's instructions. Sections were incubated in DAB solution for 10 min at room temperature, washed under running water, and then dehydration, clearing, and coverslipping were performed. Images were taken with the Mantra™ Quantitative Pathology Imaging System (PerkinElmer Inc., Waltham, Massachusetts) and cell counting in both the alveoli and interstitium was automated using the InForm® 2.4.10 software (Akoya Biosciences, Inc., Menlo Park, California). From each section, we randomly selected five images immunostained with anti-cleaved caspase-3 antibody and took them at 400× magnification. The InForm® software utilizes an automated, trainable algorithm that allows it to distinguish and identify cleaved caspase-3-positive cells as apoptotic. For this purpose, the software was trained to recognize cell nuclei through hematoxylin staining, while DAB staining was used to make the immunostaining observable. This approach allowed us to accurately evaluate a large number of images without the bias inherent in human visual analysis.

Table 1
Primer summary.

Gene	Primer sequences	
IL6	Forward	GAGGATACCACTCCCAACAGACC
	Reverse	AAGTGCATCATCGTTGTTCATACA
CD14	Forward	TTGAACCTCCGCAACGTGTCGT
	Reverse	CGCAGGAAAAGTTGAGCGAGTG
IκBα	Forward	GCCAGGAATTGCTGAGGCACTT
	Reverse	GTCTGCGTCAAGACTGCTACAC
p16/Ink4a	Forward	CCCAACGCCCCGAACT
	Reverse	GCAGAAGAGCTGCTACGTGAA
p21	Forward	CGAGAACGGTGGAACTTTGAC
	Reverse	CAGGGCTCAGGTAGACCTTG
CXCL2	Forward	CCAACCACCAGGCTACAGG
	Reverse	GCGTCACACTCAAGCTCTG
MMP3	Forward	ACATGGAGACTTTGTCCCTTTTG
	Reverse	TTGGCTGAGTGGTAGAGTCCC
ARG1	Forward	CAGAAGAATGGAAGAGTCAG
	Reverse	CAGATATGCAGGGAGTCACC
RPL4	Forward	GCCAAGACTATGCGCAGGAAT
	Reverse	GTAGCTGCTGCTTCCAGCTT

2.8. Statistics

Statistical analysis was performed using IBM SPSS Statistics version 23.0 (IBM, Armonk, New York). In order to compare the distributions of categorical variables between two or more groups, a chi-square test of independence was performed (analysis of mortality after 24 h and moving distance). To compare continuous normal distribution data between two groups, an unpaired two-tailed Student's *t*-test was performed (analysis of lung injury score and apoptotic cells in lung histology). For comparing continuous non-normal distribution data among three or more groups, the Kruskal-Wallis test followed by Dunn's multiple comparison test was employed (analysis of liver enzymes and IL-6 in blood serum and mRNA expression in lung and liver tissue). All values are presented as mean ± 95 % confidence interval (CI). Results were considered significant at $p < 0.05$.

3. Results

3.1. Hydrogen gas inhalation improved prognosis and mitigated decrease in moving distance

To evaluate the protective effect of hydrogen gas inhalation, survival and activity levels were investigated. The 24-hour survivals of each group (C, SA, SH, LA, LH1h, LH 6 h, LH1%, and LH, Fig. 1A) were 100 %, 100 %, 100 %, 78 %, 79 %, 86 %, 93 %, and 95 %, respectively (LA vs. LH, $p < 0.05$). There were no survival differences among the groups until six hours, after which survival in the LA group decreased (Fig. 1B). LPS-treated mice displayed sickness behaviors, characterized by decreased mobility. We measured the distances traveled by mice in the group (Fig. 1C). Rates of moving distance <29 cm per minute in the LA group and LH group were 43 % and 16 %, respectively, and this difference was statistically significant ($p < 0.01$). Rates of moving distance of >60 cm per minute in the LA group and LH group were 14 % and 43 %, respectively, and this difference was also statistically significant ($p < 0.01$). Prognosis and moving distance showed that the decrease due to LPS administration was reduced with the longer duration of hydrogen

administration in a day. There wasn't a large difference between the groups receiving hydrogen concentrations of 1 % and 2 %.

3.2. Hydrogen gas inhalation ameliorated mRNA expression of inflammatory biomarkers in both lung and liver tissue and reduced IL6 level in the blood serum

The extent of inflammation was assessed by the level of the pro-inflammatory cytokine IL-6 in blood serum and by the mRNA expressions of the inflammatory biomarkers IL-6, CD14, and IκBα in lung and liver tissues (Fig. 2). IL6 level in blood serum was increased by LPS administration (C: 55 pg/mL, SA: 106 pg/mL, SH: 144 pg/mL, LA: 6440 pg/mL), which was decreased by hydrogen gas inhalation with the longer duration of inhalation (LH1h: 6550 pg/mL, LH6h: 5200 pg/mL, LH: 2680 pg/mL, LA vs. LH $p < 0.01$, LH1h vs. LH $p = 0.08$, LH6h vs. LH $p < 0.01$). There was no significant difference between the groups receiving 1 % and 2 % concentrations (LH1%: 4479 pg/mL, LH: 2680 pg/mL). The mRNA expression of cytokine IL6 in lung tissue was increased by LPS administration (LA: 43.92-fold) compared to control, which was decreased with hydrogen gas inhalation as the inhalation duration (LH1h: 34.59-fold, LH6h: 26.41-fold, LH: 13.35-fold, LA vs. LH: $p < 0.01$, LH1h vs. LH: $p < 0.01$, LH6h vs. LH: $p < 0.01$). There was no significant difference between the groups receiving 1 % and 2 % concentrations (LH1%: 18.75-fold, LH: 13.35-fold). The mRNA expression level of IL6 in liver tissue was increased by LPS administration (LA: 15.44-fold) compared to control, which was decreased by hydrogen gas inhalation (LH: 8.16-fold, LA vs. LH: $p < 0.05$). However, 1 % hydrogen gas inhalation did not reduce the mRNA expression of IL6 (LH1%: 21.79-fold, LH: 8.16-fold, LH1% vs. LH: $p < 0.05$).

The mRNA expression of LPS receptor protein CD14 in lung tissue was likewise increased by LPS administration (LA: 5.82-fold) compared to control, which was suppressed by hydrogen gas inhalation with the longer inhalation duration (LH1h: 5.61-fold, LH6h: 4.96-fold, LH: 3.69-fold, LA vs. LH: $p < 0.01$, LH1h vs. LH: $p = 0.08$). There was no difference between the groups receiving 1 % and 2 % hydrogen concentration (LH1%: 3.84-fold, LH: 3.69-fold). The mRNA expression of CD14 in liver tissue was increased by LPS administration (LA: 28.96-fold) compared to control, which was suppressed by hydrogen gas inhalation (LH: 12.31, LA vs. LH: $p < 0.01$).

The mRNA expression of the NFκB signal pathway-associated molecule IκBα in lung tissue was increased by LPS administration (LA: 2.16-fold) compared to control, which was reduced by hydrogen gas inhalation (LH: 1.81-fold, LA vs LH: $p < 0.05$). However, the mRNA expression of IκBα in liver tissue was not increased by 1.25 mg/kg LPS intraperitoneal injection (LA: 1.05-fold).

3.3. Hydrogen gas inhalation alleviated lung injury in histological finding

Acute lung injury induced by LPS administration was assessed using histological assessments, which included HE staining, IL6 immunostaining, and cleaved caspase-3 immunostaining, which visualized apoptotic cells (Fig. 3A). HE staining showed that LPS 1.25 mg/kg peritoneal injection induced edema of the alveolar interstitium, migration of immune cells, protein-rich secretions in alveoli, and pulmonary congestion with small alveolar hemorrhage in the lung section. These appearances were mitigated by hydrogen gas inhalation. This finding was quantified by the lung injury score (Belperio et al., 2002), which was 4.0 [95%CI: 3.1–4.9] points in the LPS administration group, whereas hydrogen administration significantly reduced it to 1.3 [95%CI: 1.0–1.7] points (LA vs. LH: $p < 0.01$) (Fig. 3B).

IL6 immunostaining showed that the IL6-producing cells seemed to be mainly alveolar macrophages and that there were fewer IL6-positive cells in the hydrogen gas inhalation group. Immunostaining of cleaved caspase-3 was assessed for identification of apoptotic cells, which showed the number of positive cells was increased with LPS administration and mitigated with hydrogen gas inhalation. This finding was quantified by the positive cell count divided by total cells; there were more in the LA group (6.8 %) than in the LH group (0.6 %, $p < 0.01$)

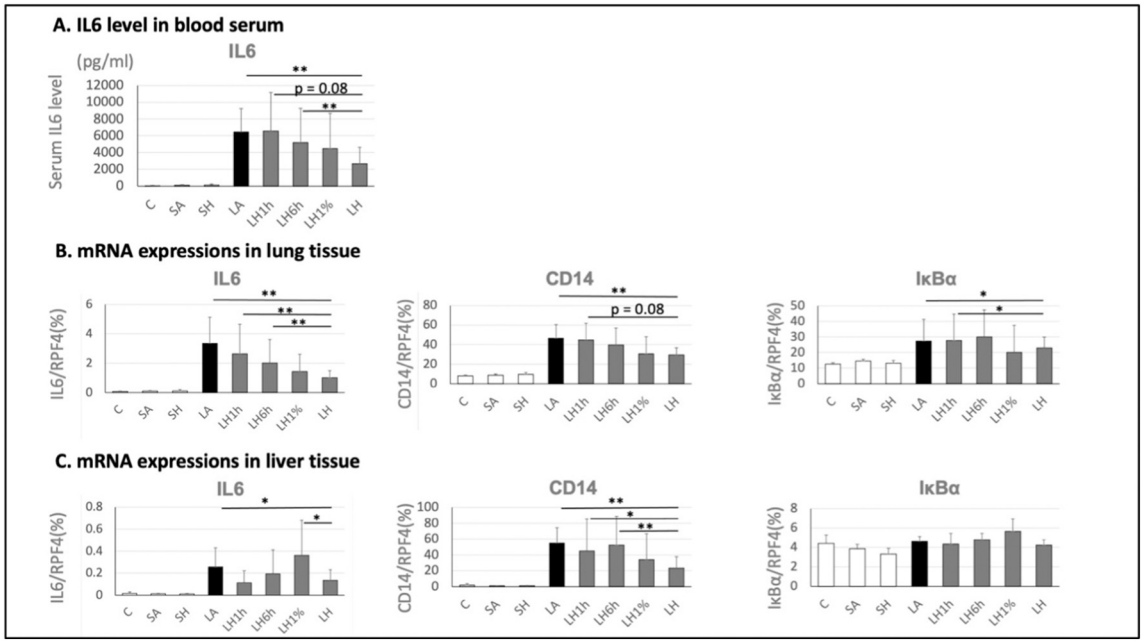

Fig. 2. Inflammation levels in blood, liver, and lungs under hydrogen gas inhalation in aged LPS-induced inflammation mice.
(A) Interleukin-6 (IL6) level in blood serum under various conditions of hydrogen gas inhalation. LH was significantly lower than LA (**$p < 0.01$) and LH6h (**$p < 0.01$). (B) RNA expressions of IL6, CD14, and IκBα in lung tissue. Expression of IL6 in LH was significantly lower than that in LA (**$p < 0.01$), LH1h (**$p < 0.01$) and LH6h (**$p < 0.01$). The expression of CD14 in LH was significantly lower than that in LA (**$p < 0.01$). The expression of IκBα in LH was significantly lower than that in LA (*$p < 0.05$) and LH1h (*$p < 0.05$). (C) Messenger RNA (mRNA) expressions of IL6, CD14, and IκBα in liver tissue. Expression of IL6 in LH was significantly lower than that in LA (*$p < 0.05$) and LH1% (* $p < 0.05$). Expression of CD14 in LH was significantly lower than that in LA (**$p < 0.01$), LA (*$p < 0.05$), and LA (**$p < 0.01$). There was no difference in the expression of IκBα among the groups.

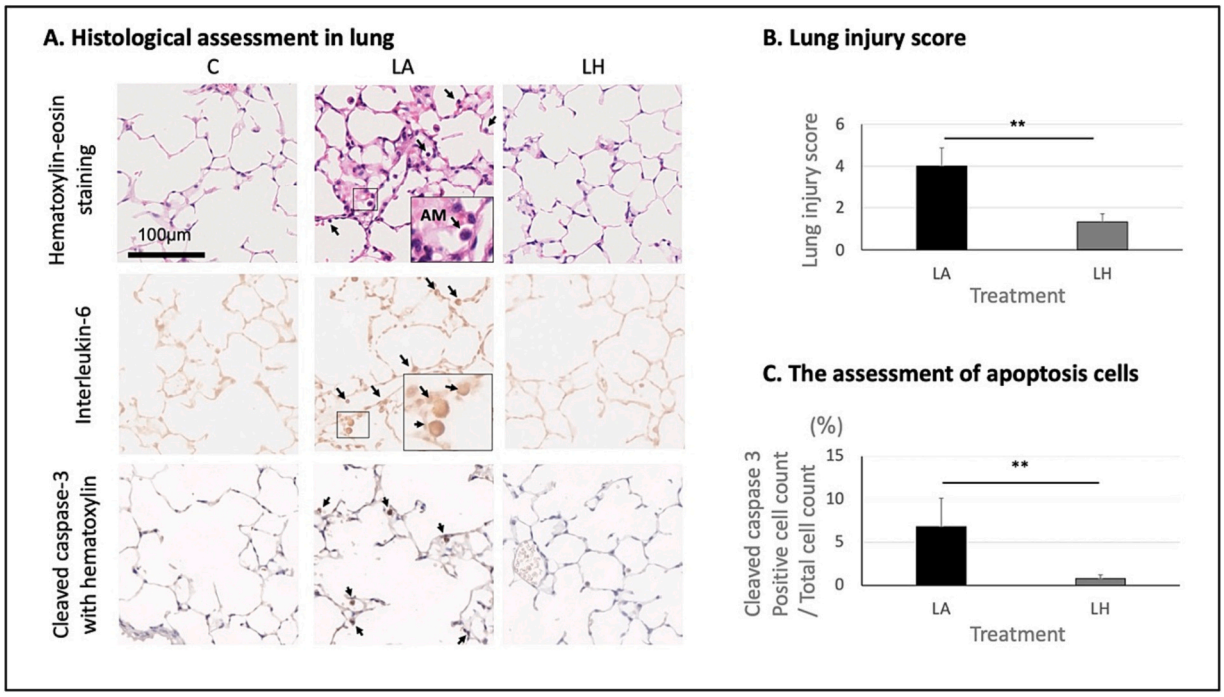

Fig. 3. Assessment of lung injury with hydrogen gas inhalation in aged LPS-induced inflammation mice.
(A) Hematoxylin and eosin (HE) staining at 24 h after LPS administration (upper A). More alveolar macrophages (AM) emerged in the alveolar space (black arrow) in the LA group than in the LH group. Protein-rich excretion, small hemorrhage, and alveolar interstitium septum thickening were evident in LA. Interleukin-6 immunostaining shows some positive cells (black arrow), identified as alveolar macrophages (middle A) via HE, in the alveolar space in LA. Cleaved caspase-3 immunostaining showed more apoptotic cells in LA than LH (black arrow). (B) Lung injury score in LA was significantly higher than that in LH (**$p < 0.01$). (C) The percentage of cleaved-caspase-3 positive cells per total cells was significantly higher in LA than in LH (**$p < 0.01$).

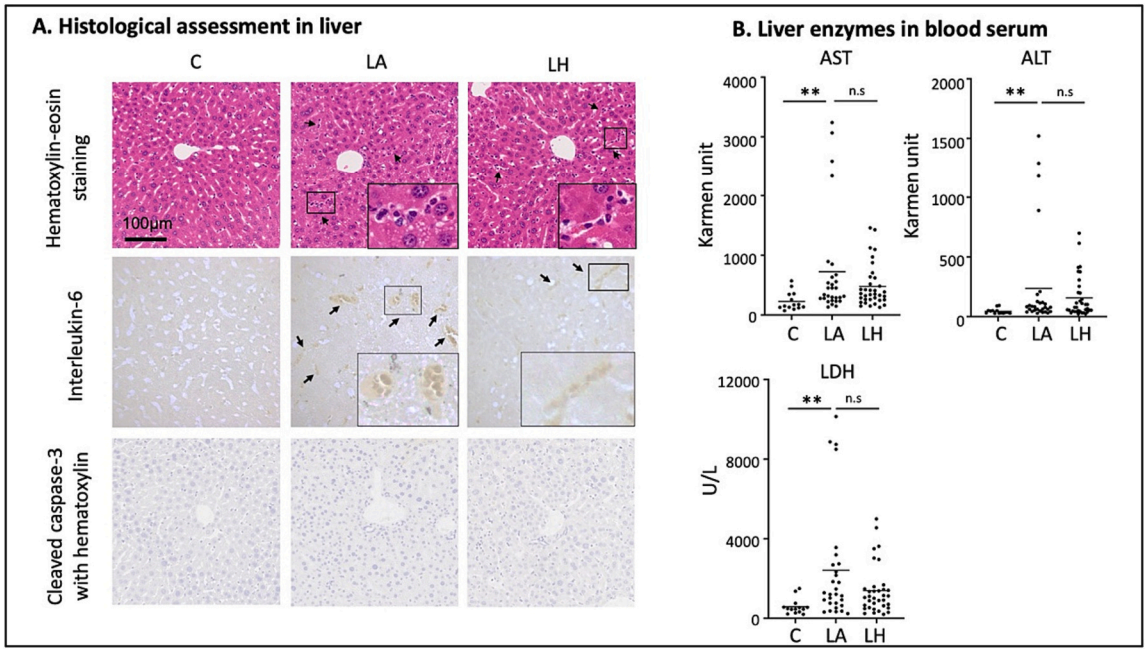

Fig. 4. Assessment of liver injury with hydrogen gas inhalation in aged LPS-induced inflammation mice.
(A) Hematoxylin and eosin (HE) staining at 24 h after LPS administration (upper A). No hepatic mesenchymal injury was found in LA and LH. In the hepatic sinusoids, accumulation of immune cells (black arrow) was found in both LA and LH (upper A). Interleukin-6 immunostaining shows some positive cells (black arrow) in the hepatic sinusoids, where immune cells were identified using HE staining. Few apoptotic cells were found in both LA and LH. (B) Aspartate aminotransferase (AST), alanine aminotransferase (ALT), and lactate dehydrogenase (LDH) were significantly higher in LA than C (**$p < 0.01$); however, there are no differences in these levels between LA and LH.

(Fig. 3C).

3.4. Hydrogen gas inhalation did not alleviate LPS-induced liver injury under the tested conditions

Hepatic histology was evaluated to assess tissue changes and the effect of hydrogen on LPS administration (Fig. 4A). No changes in the hepatic parenchyma were observed under the condition of 1.25 mg/kg LPS intraperitoneal administration. Immune cell accumulation in the hepatic sinusoids was observed in both the LA and LH groups. Immunostaining for cleaved caspase-3 to identify apoptotic cells showed few positive cells among the control group, LA group, and LH group.

Immunostaining for IL6 was also performed to identify the site of IL6 expression in LPS-treated liver tissue. The site of IL6-positive cell expression was consistent with the accumulation of immune cells in the hepatic sinusoids seen in HE staining.

Liver enzymes in the blood serum were analyzed to assess liver injury by LPS treatment (Fig. 4B). AST, ALT, and LDH were increased by LPS treatment (AST C: 114 Karmen unit [95 % CI:70–159], LA: 363 Karmen unit [95 % CI:196–530] $p < 0.01$, ALT C: 45 Karmen unit [95 % CI:33–58], LA: 237 Karmen unit [95 % CI:80–393] $p < 0.01$, LDH C: 291 IU/L [95 % CI:179–403], LA: 1208 IU/L [95 % CI: 665–1750] $p < 0.01$); however, hydrogen gas inhalation did not mitigate the values of those enzymes (AST LH: 241 Karmen unit [95 % CI: 180–301], ALT LH: 157 Karmen unit [95 % CI: 98–217], LDH LH: 695 IU/L [95 % CI: 485–904]).

3.5. Hydrogen gas inhalation attenuated the expression of p21, CXCL2, and MMP3 in lung tissue

To confirm the expression of genes associated with tissue senescence, mRNA expression of p16/Ink4a, p21, CXCL2, and MMP3 was evaluated. p21 is a strong cyclin-dependent kinase inhibitor that inhibits cell cycle progression. It is an important signaling protein in cellular senescence but is also known to be sensitive to stress responses (stress-induced cellular senescence). CXCL2 is chemokine generally secreted from immune and vascular endothelial cells, and MMP3 is a protein associated with tissue remodeling in arthritis and tumor metastasis. Both are also known to be secreted from senescent cells. Expressions of p21, CXCL2, and MMP3, which were enhanced by LPS administration (p21 LA: 2.82-fold, CXCL2 LA: 36.1-fold, MMP3 LA: 4.01-fold, compared to control), were attenuated by hydrogen gas inhalation (p21 LH: 2.26-fold, $p < 0.05$, CXCL2 LH: 18.3-fold, $p < 0.05$, MMP3 LH: 3.09-fold, $p < 0.05$) (Fig. 5).

ARG1 is a protein secreted by macrophages in response to oxidative stress and catalyzes glutamine metabolism, thereby suppressing nitric oxide production and consequently reducing inflammation. The expression of ARG1 mRNA was upregulated by LPS administration (LA: 52.7-fold compared to control). While not reaching statistical significance, a trend toward amelioration was observed with hydrogen gas inhalation (LH: 18.3-fold, $p = 0.054$).

3.6. Hydrogen gas inhalation attenuated the expression of p21; however, it did not attenuate the expression of CXCL2, MMP3, and ARG1 in liver tissue

We assessed the upregulation of p16/Ink4a, p21, CXCL2, MMP3, and ARG1 expression, which was observed in lung tissue, to determine if it was observed in liver tissue as well (Fig. 6). mRNA expression of p21 was elevated by LPS administration (LA: 4.27-fold compared to control), which was reduced by hydrogen gas inhalation (LH: 2.58-fold, $p < 0.01$). The mRNA expressions of CXCL2, MMP3, and ARG1 were elevated by LPS administration (CXCL2 LA: 10.8-fold, MMP3 LA: 13.7-fold, ARG1 LA: 1.91-fold compared to control); however, hydrogen gas inhalation did not reduce these expressions (CXCL2 LH: 15.3-fold, MMP3 LH: 11.7-fold, ARG1 LH:1.54-fold).

4. Discussion

This study demonstrated that hydrogen gas inhalation improved the survival rate and activity level in an elderly LPS-induced inflammation model, which was induced by intraperitoneal injection of 1.25 mg/kg in mice aged 21 to 23 months. While the focus on the elderly in this model is critical due to the global growth in the aging population and their particular susceptibility to sepsis as a result of immunosenescence (aging of the immune system) and cellular senescence (biological aging of cells), it's essential to recognize that this study focuses on a sterile inflammation model, and therefore cannot be directly applied to infection-mediated sepsis. Nevertheless, the significant improvement in prognosis brought about by hydrogen gas inhalation in our elderly LPS-induced inflammation model holds promise for future medical applications in treating sepsis among the elderly, thus addressing a substantial public health challenge.

Second, this study clarified the duration and concentration of hydrogen gas inhalation needed to achieve an anti-inflammatory effect. It has been suggested that the duration and concentration of hydrogen gas administration may vary depending on the target organ, while at

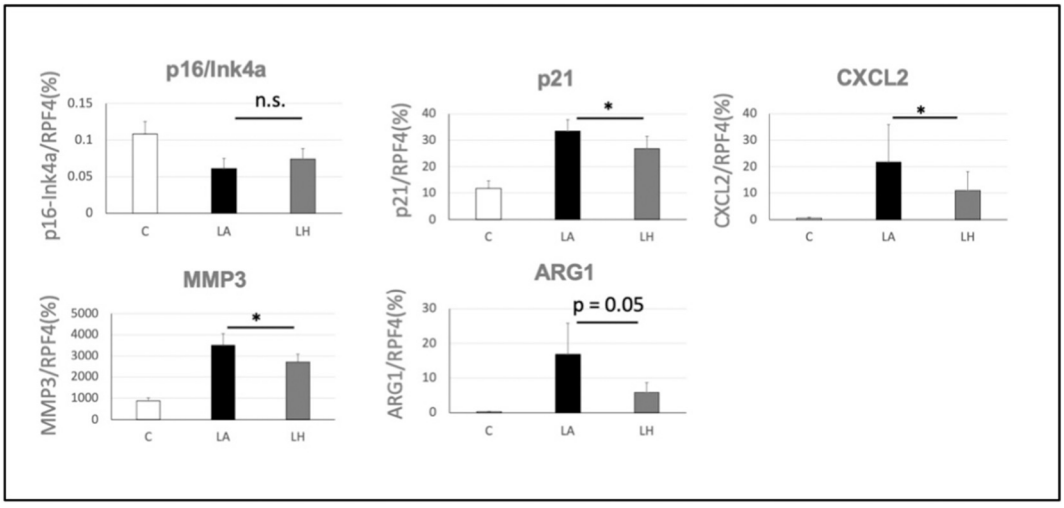

Fig. 5. mRNA expressions of p21, MMP3, CXCL2, and ARG1 in lung tissue.
mRNA expressions of p16/Ink4a, p21, C-X-C motif chemokine 2 (CXCL2), metalloproteinase-3 (MMP3), and arginase-1 (ARG1) in lung tissue. These expressions were significantly higher in LA than in LA (*$p < 0.05$). There were no differences in p16/Ink4a.

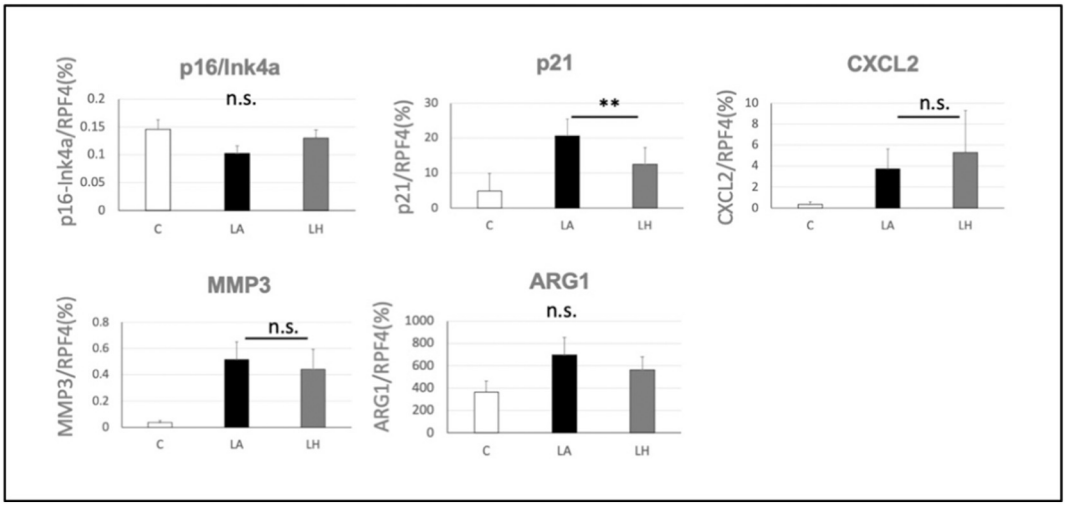

Fig. 6. mRNA expressions of p21, MMP3, CXCL2, and ARG1 in liver tissue.
mRNA expressions of p16/Ink4a, p21, CXCL2, MMP3, and ARG1 in liver tissue. Expression of p21 was significantly higher in LA than in LA (*$p < 0.05$). There were no differences in p16/Ink4a, CXCL2, MMP3, and ARG1.

least 2 % and continuous inhalation proved appropriate for lung inflammation and injury. Hydrogen gas is flammable at concentrations above 4.1 % (*Safety Standard for Hydrogen and Hydrogen Systems: Guidelines for Hydrogen System Design, Materials Selection, Operations, Storage and Transportation - NASA Technical Reports Server (NTRS),* n.d.). Considering the safety range, the maximum concentration for this study was set at 2 %. With activity level and survival as endpoints, this research revealed that the optimal concentration of hydrogen gas is 2 % and the optimal duration is continuous inhalation for 24 h. According to previous studies on the concentration of hydrogen gas inhalation, the effects of 1 %, 2 %, and 4 % concentration on cerebral infarction were compared, with the most effective concentration being 2 % (Ohsawa et al., 2007). Since then, most published studies have adopted a hydrogen gas inhalation concentration of 2 %, although no studies have been conducted on concentrations targeting anti-inflammatory effects. Optimal duration is also controversial. Gao et al. revealed that six-hour hydrogen gas inhalation reduced lung injury the most among two-hour, four-hour, and six-hour hydrogen gas inhalation in a day (Gao et al., 2019). Ito et al. showed that intermittent inhalation was more effective than continuous inhalation in a Parkinson's disease model animal (Ito et al., 2012). The optimal duration may differ depending on the target organ, type of disease (degenerative or inflammatory diseases), and disease progression speed (slow or acute progression). However, we recognize that our study has limitations due to safety and ethical constraints. Specifically, due to safety regulations in our animal experimentation facility, we could not use a mixture of hydrogen, nitrogen, and oxygen gases with hydrogen concentrations higher than 2 %. Additionally, from an ethical perspective aimed at minimizing animal suffering, we limited the observation period to 24 hours post-LPS administration. As a result, there is a possibility that higher concentrations than 2 % and longer durations than 24 h might yield better outcomes, but we were unable to investigate this in our study.

Finally, this study evaluated the mRNA expression of p16/Ink4a and p21, which are senescent biomarkers that both regulate cell cycle progression. CXCL2 and MMP3 were generally secreted from immune cells, vascular endothelial cells, and fibroblasts by pro-inflammatory signaling, and it has been clear that senescent cells also secrete or induce CXCL2 and MMP3 and cause chronic inflammation, consequently leading to organ fibrosis and organ dysfunction. Therefore, these signaling proteins shape organ senescence and are referred to as senescence-associated secretory phenotypes (SASPs) (de Magalhães and Passos, 2018). Upregulation of all these mRNAs except p16/Ink4a were proven to be mitigated by hydrogen gas inhalation. This observation is paramount as it implies that hydrogen treatment may inhibit cellular senescence-associated organ aging in conditions of LPS-induced inflammation, leading to organ function preservation in elderly patients following severe inflammation. The p16/Ink4a gene is regulated by several upstream signaling pathways that are involved in growth control, cell cycle regulation, and DNA damage response, including TGF-β, Ras, ataxia telangiectasia mutated (ATM) signaling, and Notch signaling. The expression of p16/Ink4a is triggered by structural changes in chromosomes associated with cellular aging, making it a relatively slow response. Previous studies have observed an increase in p16/Ink4a expression after a period of one week to one month (Harada et al., 2021; Islam et al., 2023). In this study, we evaluated the expression after 24 h, which may too short a time period to capture changes in expression. While we were able to confirm the expression of genes indicating aging such as p21, CXCL2, and MMP3, a clear limitation of our study is that we evaluated these biomarkers in whole lung homogenates consisting of numerous different cell types. Consequently, we were unable to ascertain which specific cell types were contributing to the observed signals.

The significant limitation of this study is that the mechanism of mitigation of inflammation could not be clarified. Aged mice are not suitable for mechanistic analysis because individual variation is greater than that among young mice, and genetically engineered aged mice cannot be easily created. In addition, aged mice are easily vulnerable to surgical procedures and deep anesthesia techniques as shown by preliminary experiments. Ideally, we would have preferred to use a live bacterial infection model or a cecal ligation and puncture sepsis model; however, the creation of an appropriate model is difficult because of the need for anesthesia or surgery. As a result, we were compelled to choose a simpler model, such as intraperitoneal administration of LPS. This use of a 'sterile sepsis' model rather than live bacterial pathogens represents a limitation of our study. Another potential limitation to consider is the CO2 concentration in our sealed exposure chamber. While regular air exchanges, we acknowledge that the measured concentration of 2754 ± 302 ppm (average ± standard deviation) could be a potential stressor for the mice.

Despite the limitations of the mechanistic analysis in this study, we were able to analyze the change in mRNA expression involved in inflammatory signaling pathways related to toll-like receptor 4 (TLR4). Hydrogen suppresses the expression of CD14 and IκBα, suggesting that its reaction is related to the suppression of the inflammatory signaling pathway from where LPS binds to TLR4 receptors on immune cells to where NFκB is activated (Hashem et al., 2021). The site of this reaction

was suggested to be alveolar macrophages in the lung and the accumulation of immune cells in hepatic sinusoids in the liver because these cells were proven to produce the pro-inflammatory protein IL6 by LPS administration in immunostaining analysis. These results are compatible with the NFκB inhibitory effects of hydrogen shown in the previous hemorrhagic shock-induced lung injury experiment (Kohama et al., 2015) and the anti-inflammatory effects of hydrogen via NRF2 activation shown in the experiment using hyperoxia-induced lung injury (Kawamura et al., 2013).

However, the intraperitoneal administration of 1.25 mg /kg LPS did not cause injury to the hepatic parenchyma or hepatocytes in the histological analysis, which can make it difficult to analyze organ protection by hydrogen gas inhalation. Despite the significant elevation of liver enzymes by this LPS administration, hydrogen gas inhalation did not significantly improve them. Because in the previous experiment of 30 mg/kg LPS intraperitoneal administration in seven-week-old mice, it was found that drinking saturated hydrogenated water mitigated liver injury (Iketani et al., 2017), the inhalation method may have less of an effect than drinking saturated hydrogenated water. An equivalent LPS dose could not be used in this study because aged mice were so vulnerable that the mortality in 24 h is 40 % with 10 mg/kg administration. In order to identify the appropriate dose for aged mice, we conducted preliminary experiments to find the LPS dose that would result in a survival rate of about 80 %, which revealed that 1.25 mg/kg was appropriate and chosen as the dose for this study (data not shown).

From the limited data available, we focused on inflammation in the liver and found that LPS administration induces inflammatory cells to cluster in the hepatic sinusoids where IL6 is produced. Furthermore, mRNA expression showed that inhalation of hydrogen gas alleviated the increase in IL6 production. Interestingly, in the liver, IL6 did not decrease with 1 % hydrogen gas inhalation, contrary to findings in the lungs. This suggests that the hydrogen administration method may need to be modified depending on the injured organ. With hydrogenated water drinking, absorbed molecular hydrogen in the intestines can pass the portal vein by blood flow toward the liver (Ichihara et al., 2021). In hydrogen gas inhalation, molecular hydrogen comes in direct contact with alveolar epithelial cells and alveolar macrophages through the trachea and bronchus; then hydrogen gas is absorbed into the vessel and circulates throughout the organs (Sano et al., 2020). However, the previous study showed that hydrogen was diluted or diffused during blood circulation, and hydrogen concentrations in the portal vein were below detection sensitivity (Sano et al., 2020). Namely, in hydrogen gas inhalation, the organs with the highest concentration absorbed by cells are the lungs and there is less concentration in the liver.

In a significant advance in our understanding, we have demonstrated that hydrogen gas mitigates LPS-induced inflammation even in aged mice, which present unique patterns of inflammation parameters, such as chronic inflammation and aging immunity. Our findings here extend beyond the results of previous studies that employed younger mice. Importantly, we discovered that hydrogen gas inhalation exerts significant effects particularly in the lungs. This novel insight offers an additional perspective to the existing body of research, underlining the potential of hydrogen gas in treating inflammation-related conditions in aged individuals.

5. Conclusion

Our elderly LPS-induced inflammation mouse model demonstrates the potential role of hydrogen gas in modulating not only inflammation but also cellular senescence, which is particularly relevant to aging. The inhalation of 2 % hydrogen gas effectively reduced inflammation in both the lung and liver, mitigated lung injury, and ultimately led to improved survival rates and activity levels. These findings pave the way for developing interventions that are tailored to the multifaceted nature of sepsis in the elderly population and highlight the necessity for further investigations into the interplay between aging, cellular senescence, and inflammation.

List of abbreviations

Alanine aminotransferase, ALT; Arginase-1, ARG1; Aspartate aminotransferase, AST; ataxia telangiectasia mutated, ATM; Confidence interval, CI; C-X-C motif chemokine 2, CXCL2; Hematoxylin and eosin, HE; Interleukin-6, IL6; Metalloproteinase-3, MMP3; Messenger RNA, mRNA; Lipopolysaccharide, LPS; Phosphate buffered saline, PBS; Polymerase chain reaction, PCR; Ribosomal protein L4, RPL4; Tris buffered saline with 0.1 % Tween 20, TBS-T; The control group, C group; The saline administration and non-hydrogen treatment group, SA group; The saline administration and 2 % hydrogen treatment group, SH group; The LPS administration and non-hydrogen treatment group, LA group; The LPS administration and 2 % hydrogen treatment group, LH group; The LPS administration and six-hour hydrogen treatment group, LH6h group; The LPS administration and one-hour hydrogen treatment group, LH1h group; The LPS administration and 1 % hydrogen treatment group, LH1 % group.

Ethics approval and consent to participate

All protocols followed the principles of laboratory animal care (NIH Publication No. 86-23, revised 1985), and all research protocols were reviewed and approved by the Animal Care and Use Committee of the Tokyo Metropolitan Institute of Gerontology (No.19009, No.22001). This study was conducted in compliance with the ARRIVE guidelines (https://arriveguidelines.org/).

Consent for publication

Not applicable.

Availability of data and materials

All data generated or analyzed during the current study are included in this article.

CRediT authorship contribution statement

Toshiyuki Aokage: Conceptualization, Methodology, Writing – original draft. **Masumi Iketani:** Methodology. **Mizuki Seya:** Methodology. **Ying Meng:** Methodology. **Kohei Ageta:** Visualization, Writing – review & editing. **Hiromichi Naito:** Supervision. **Atsunori Nakao:** Project administration. **Ikuroh Ohsawa:** Project administration, Funding acquisition.

Declaration of competing interest

The authors declare that they have no competing interests.

Acknowledgements

The authors thank Christine Burr for editing the manuscript.

This study was supported by a grant from the Japan Society for the Promotion of Science Grants-in-Aid for Scientific Research (JSPS KAKENHI), Grant Number: 22K09162 and Tokyo Metropolitan Institute of Gerontology Grants for Translational Research.

References

Accardi, G., Caruso, C., 2018. Immune-inflammatory responses in the elderly: an update. Immun. Ageing 15. https://doi.org/10.1186/S12979-018-0117-8.

Aokage, T., Seya, M., Hirayama, T., Nojima, T., Iketani, M., Ishikawa, M., Terasaki, Y., Taniguchi, A., Miyahara, N., Nakao, A., Ohsawa, I., Naito, H., 2021. The effects of inhaling hydrogen gas on macrophage polarization, fibrosis, and lung function in

mice with bleomycin-induced lung injury. BMC Pulm. Med. 21 https://doi.org/10.1186/S12890-021-01712-2.
Belperio, J.A., Keane, M.P., Burdick, M.D., Londhe, V., Xue, Y.Y., Li, K., Phillips, R.J., Strieter, R.M., 2002. Critical role for CXCR2 and CXCR2 ligands during the pathogenesis of ventilator-induced lung injury. J. Clin. Invest. 110, 1703–1716. https://doi.org/10.1172/JCI15849.
de Magalhães, J.P., Passos, J.F., 2018. Stress, cell senescence and organismal ageing. Mech. Ageing Dev. 170, 2–9. https://doi.org/10.1016/J.MAD.2017.07.001.
Dumont, P., Balbeur, L., Remacle, J., Toussaint, O., 2000. Appearance of biomarkers of in vitro ageing after successive stimulation of WI-38 fibroblasts with IL-1alpha and TNF-alpha: senescence associated beta-galactosidase activity and morphotype transition. J. Anat. 197 (Pt 4), 529–537. https://doi.org/10.1046/J.1469-7580.2000.19740529.X.
Franceschi, C., Campisi, J., 2014. Chronic inflammation (Inflammaging) and its potential contribution to age-associated diseases. J. Gerontol. A Biol. Sci. Med. Sci. 69, S4–S9. https://doi.org/10.1093/gerona/glu057.
Gao, L., Jiang, D., Geng, J., Dong, R., Dai, H., 2019. Hydrogen inhalation attenuated bleomycin-induced pulmonary fibrosis by inhibiting transforming growth factor-β1 and relevant oxidative stress and epithelial-to-mesenchymal transition. Exp. Physiol. 104, 1942–1951. https://doi.org/10.1113/EP088028.
Harada, T., Tsuboi, I., Hino, H., Yuda, M., Hirabayashi, Y., Hirai, S., Aizawa, S., 2021. Age-related exacerbation of hematopoietic organ damage induced by systemic hyper-inflammation in senescence-accelerated mice. Sci. Rep. 11 https://doi.org/10.1038/S41598-021-02621-4.
Hashem, H.E., Ibrahim, Z.H., Ahmed, W.O., 2021. Diagnostic, prognostic, predictive, and monitoring role of neutrophil CD11b and monocyte CD14 in neonatal sepsis. Dis. Markers 2021. https://doi.org/10.1155/2021/4537760.
Ichihara, G., Katsumata, Y., Moriyama, H., Kitakata, H., Hirai, A., Momoi, M., Ko, S., Shinya, Y., Kinouchi, K., Kobayashi, E., Sano, M., 2021. Pharmacokinetics of hydrogen after ingesting a hydrogen-rich solution: a study in pigs. Heliyon 7. https://doi.org/10.1016/J.HELIYON.2021.E08359.
Iketani, M., Ohshiro, J., Urushibara, T., Takahashi, M., Arai, T., Kawaguchi, H., Ohsawa, I., 2017. Preadministration of hydrogen-rich water protects against lipopolysaccharide-induced sepsis and attenuates liver injury. Shock 48, 85–93. https://doi.org/10.1097/SHK.0000000000000810.
Imaeda, T., Nakada, T. aki, Takahashi, N., Yamao, Y., Nakagawa, S., Ogura, H., Shime, N., Umemura, Y., Matsushima, A., Fushimi, K., 2021. Trends in the incidence and outcome of sepsis using data from a Japanese nationwide medical claims database-the Japan Sepsis Alliance (JaSA) study group. Crit. Care 25. https://doi.org/10.1186/S13054-021-03762-8.
Islam, M.T., Tuday, E., Allen, S., Kim, J., Trott, D.W., Holland, W.L., Donato, A.J., Lesniewski, L.A., 2023. Senolytic drugs, dasatinib and quercetin, attenuate adipose tissue inflammation, and ameliorate metabolic function in old age. Aging Cell 22. https://doi.org/10.1111/ACEL.13767.
Ito, Mikako, Hirayama, M., Yamai, K., Goto, S., Ito, Masafumi, Ichihara, M., Ohno, K., 2012. Drinking hydrogen water and intermittent hydrogen gas exposure, but not lactulose or continuous hydrogen gas exposure, prevent 6-hydorxydopamine-induced Parkinson's disease in rats. Med. Gas Res. 2, 15. https://doi.org/10.1186/2045-9912-2-15.
Kawai, S., Takagi, Y., Kaneko, S., Kurosawa, T., 2011. Effect of three types of mixed anesthetic agents alternate to ketamine in mice. Exp. Anim. 60, 481–487. https://doi.org/10.1538/EXPANIM.60.481.
Kawamura, T., Wakabayashi, N., Shigemura, N., Huang, C.S., Masutani, K., Tanaka, Y., Noda, K., Peng, X., Takahashi, T., Billiar, T.R., Okumura, M., Toyoda, Y., Kensler, T. W., Nakao, A., 2013. Hydrogen gas reduces hyperoxic lung injury via the Nrf2 pathway in vivo. Am. J. Physiol. Lung Cell. Mol. Physiol. 304 https://doi.org/10.1152/AJPLUNG.00164.2012.
Kohama, K., Yamashita, H., Aoyama-Ishikawa, M., Takahashi, T., Billiar, T.R., Nishimura, T., Kotani, J., Nakao, A., 2015. Hydrogen inhalation protects against acute lung injury induced by hemorrhagic shock and resuscitation. Surgery 158, 399–407. https://doi.org/10.1016/J.SURG.2015.03.038.
Kotfis, K., Wittebole, X., Jaschinski, U., Solé-Violán, J., Kashyap, R., Leone, M., Nanchal, R., Fontes, L.E., Sakr, Y., Vincent, J.L., 2019. A worldwide perspective of sepsis epidemiology and survival according to age: observational data from the ICON audit. J. Crit. Care 51, 122–132. https://doi.org/10.1016/J.JCRC.2019.02.015.
Ohsawa, I., Ishikawa, M., Takahashi, K., Watanabe, M., Nishimaki, K., Yamagata, K., Katsura, K.I., Katayama, Y., Asoh, S., Ohta, S., 2007. Hydrogen acts as a therapeutic antioxidant by selectively reducing cytotoxic oxygen radicals. Nat. Med. 13, 688–694. https://doi.org/10.1038/NM1577.
Safety Standard for Hydrogen and Hydrogen Systems: Guidelines for Hydrogen System Design, Materials Selection, Operations, Storage and Transportation - NASA Technical Reports Server (NTRS) [WWW Document], n.d. URL https://ntrs.nasa.gov/citations/19970033338 (accessed 5.6.23).
Sano, M., Ichihara, G., Katsumata, Y., Hiraide, T., Hirai, A., Momoi, M., Tamura, T., Ohata, S., Kobayashi, E., 2020. Pharmacokinetics of a single inhalation of hydrogen gas in pigs. PLoS One 15. https://doi.org/10.1371/JOURNAL.PONE.0234626.
Venkatesh, B., Finfer, S., Cohen, J., Rajbhandari, D., Arabi, Y., Bellomo, R., Billot, L., Correa, M., Glass, P., Harward, M., Joyce, C., Li, Q., McArthur, C., Perner, A., Rhodes, A., Thompson, K., Webb, S., Myburgh, J., 2018. Adjunctive glucocorticoid therapy in patients with septic shock. N. Engl. J. Med. 378, 797–808. https://doi.org/10.1056/NEJMOA1705835.
Yamamoto, H., Aokage, T., Igawa, T., Hirayama, T., Seya, M., Ishikawa-Aoyama, M., Nojima, T., Nakao, A., Naito, H., 2020. Luminal preloading with hydrogen-rich saline ameliorates ischemia-reperfusion injury following intestinal transplantation in rats. Pediatr. Transplant. 24 https://doi.org/10.1111/PETR.13848.